Inelastic Scattering of the NCO($X^2\Pi$) Radical with the He Atom on an *Ab Initio* Potential Energy Surface†

J. Kłos*

Department of Chemistry and Biochemistry, University of Maryland, College Park, Maryland 20742, and Departamento de Química Física I, Facultad de Química Universidad Complutense, 28040 Madrid, Spain

R. Toboła and G. Chałasiński

Faculty of Chemistry, University of Warsaw, Pasteura 1, 02-093 Warszawa, Poland

Received: April 28, 2009; Revised Manuscript Received: July 7, 2009

The $^2A'$ and $^2A''$ adiabatic potential energy surfaces for the He−NCO($X^2\Pi$) van der Waals system are obtained by the partially spin-restricted coupled cluster method with single, double, and noniterated triple excitations (RCCSD(T)). The *ab initio* potentials are fit to analytical expressions, and scattering and bound state calculations are performed for a rigid NCO($^2\Pi$) radical. Rotational constants of the complex are reported. The scattering calculations of integral and differential cross sections are performed using both the fully quantum close-coupling (CC) and coupled-states (CS) methods. The collision energies have the values taken from the experiment of Macdonald and Liu (*J. Chem. Phys.* **1992**, *97*, 978). The excellent agreement between theoretical and experimental scattering results attests good quality of the *ab initio* potential.

I. Introduction

Modeling of scattering processes of open-shell radicals with closed-shell targets is particularly important from the point of view of atmospheric chemistry[1,2] and astrophysics of interstellar clouds that abound with diatomic radicals such as OH($^2\Pi$),[3] CN($^2\Sigma$),[4] and NO($^2\Pi$).[5,6] The triatomic NCO($X^2\Pi$) radical has been studied before in the connection of its presence in the dark dense interstellar clouds),[7,8] but also as an intermediate species in combustion chemistry of compounds containing nitrogen.[9−11] There are many theoretical studies of the NCO($X^2\Pi$) molecule and its hyperfine, vibronic and spin−orbit structure (see refs 12, 13 and references therein). To the best of our knowledge, there are no previous reports of theoretical calculations of interaction energy of the NCO($^2\Pi$) molecule with rare gas atoms. There are several experimental studies of the inelastic scattering of NCO with He atoms reported by Macdonald and Liu[14−16] as well as for the Ar−NCO system by Liu and coworkers.[17] The state-resolved integral cross sections in a crossed-beam apparatus for inelastic scattering with He atoms has been measured.[14] The authors report inelastic cross sections in relative units for the range of collision energies of 328.77 cm^{-1}, 566.60 cm^{-1}, 828.92 cm^{-1}, and 1066.75 cm^{-1}. The results of Macdonald et al. are resolved for final spin−orbit states as well as for Λ-doublet splittings. The dependence of selected cross sections on the collision energy has also been shown.

In this paper we report the state-of-the-art *ab initio* calculations of the interaction energy between the NCO($^2\Pi$) radical and the He atom. The *ab initio* points are used to obtain analytical representation of the adiabatic and diabatic potentials. The potentials are subsequently applied in the fully quantum close-coupling and coupled-states calculations to obtain state-resolved integral and differential cross sections for a range of collision energies corresponding to the experiment of Macdonald and Liu.[14] In addition, the coupled-states approximation calculations are used to scan the collision energy dependence of the integral cross sections on a finer grid of energies. We compare our theoretical scattering results with the experimental results of Macdonald et al.[14] accordingly scaled to match the sum of the theoretical cross sections for a given collision energy.

We also perform the bound states calculations of the complex for the first few values of the total angular momentum quantum number *J*. From these calculations, we are able to estimate the values of the rotational constant of the entire complex and its zero-point corrected dissociation energy.

II. Ab Initio Calculations

To calculate interaction energy between the He atom and the NCO($^2\Pi$) radical we applied the supermolecular approach. Within the supermolecular framework the interaction energy of the open-shell system is defined as follows:

$$\Delta E_{\mathrm{int}}(Q;\Gamma) = E_{\mathrm{AB}}^{\mathrm{dcbs}}(Q;\Gamma) - E_{\mathrm{A}}^{\mathrm{dcbs}}(Q) - E_{\mathrm{B}}^{\mathrm{dcbs}}(Q;\Gamma) \quad (1)$$

where AB and B are the open-shell species and Q denotes the Jacobi coordinates of the relative position of the He atom with respect to the NCO molecule. The "dcbs" superscript stands for the dimer centered basis set. Γ denotes the symmetry of the electronic state with respect to the operation of reflection in the plane defined by the linear molecule B and an atom A. The total energies of the He atom and the NCO radical are calculated using the dimer (He−NCO) basis set. This allows us to remove basis set superposition error (BSSE) according to the counterpoise correction procedure of Boys and Bernardi.[18] We will briefly describe below the geometry of the He−NCO complex and the electronic structure methods applied in the calculations of the total energies of the dimer and monomers as well as the basis sets.

† Part of the "Vincenzo Aquilanti Festschrift".

10.1021/jp903918r
Published on Web 08/14/2009

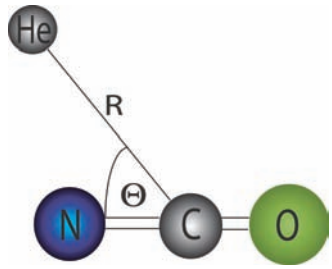

Figure 1. Schematic picture of the Jacobi coordinates used in *ab initio* calculations of the He−NCO system.

A. Geometry. To reduce the dimension of the problem we decided to treat the NCO($^2\Pi$) molecule as a rigid rotor at the equilibrium geometry. We optimized the NCO geometry at the RCCSD(T) level of theory, using an augmented correlation consistent triple-ζ (aug-cc-pvtz) basis set of Dunning.[19] In the equilibrium the NCO radical is linear with the distance between N and C $r_{NC} = 1.236$ Å, and the distance between C and O $r_{CO} = 1.184$ Å. This gives the equilibrium distance between the terminal N and O atoms of $r_e = 2.42$ Åor 4.57 a_0. The results for r_{NC} and r_{CO} are very close to the recent theoretical findings of Prasad[12] which are 1.237 Å and 1.180 Å, respectively, and also close to the experimental determination of Ramsay,[20] who reports the distances of 1.23 Å and 1.19 Å, respectively.

In Figure 1 we define the set of Jacobi coordinates $(\vec{R},\vec{r},\theta)$ with vector $\vec{r}$ lying along the axis of the NCO molecule, vector $\vec{R}$ defining the position of the He atom with respect to center of mass of the NCO molecule and the Jacobi angle θ defined as the angle between the vectors $\vec{r}$ and $\vec{R}$ with $\theta = 0$ corresponding to the collinear arrangement He···N═C═O.

The supermolecular *ab initio* calculations were performed at the discrete grid of R and θ variables. The angular grid consisted of 11 values of $\theta \in$ [0, 20, 40, 60, 80, 90, 100, 120, 140, 160, 180] degrees. The radial grid of 48 points distributed along R variable covered the short-range and the long-range regions from $R = 3.0$ a_0 to $R = 20.0$ a_0. This amounts to 528 *ab initio* points to represent 2-dimensional potential energy surface of the He−NCO complex.

B. Basis Set and *Ab Initio* Methods. The NCO($^2\Pi$) molecule is an open-shell radical with the total value of spin $S = 1/2$. The dominant electronic configuration of the $X^2\Pi$ state of the linear NCO molecule is $[1-6]\sigma^2 1\pi^4 7\sigma^2 2\pi^3$. The singly occupied molecular orbital, either π_x or π_y, determines the symmetry of the total wave function of the He−NCO system with respect to reflection operation in the supermolecular plane. When the singly occupied orbital is perpendicular to this plane, for example π_x^*, one has an electronic state of the $^2A''$ symmetry, in the other case one has a state of the $^2A'$ symmetry. For collinear arrangements, the A′ and A″ states become degenerate and correspond to the doubly degenerate Π state. These electronic states can be described by single-determinant wave functions, therefore we choose single-reference methods to calculate total energies of the dimer and monomers in eq 1. The both reference wave functions, for the dimer and monomers, are calculated within the restricted Hartree−Fock method (RHF). Using symmetry control in MOLPRO[21] suite of programs we can uniquely define which Γ symmetry of the electronic state of the dimer and NCO monomer that we want to obtain. For the counterpoise correction this symmetry must be the same for both the open-shell supermolecule and the open-shell monomer.

The partially spin-restricted coupled cluster method with single, double, and noniterated triple excitations (RCCSD(T)) is applied to calculate the adiabatic A′ and A″ potential energy surfaces. The reference orbitals are taken from the RHF calculations.

We used the aug-cc-pvtz basis set with the additional set of 3s2p2d2f1g bond functions placed halfway between He and the center of mass of NCO. Bond functions proved to be useful in recovering significant part of the dispersion component of the interaction energy.[22]

III. Modeling of the PES

To use the *ab initio* potentials in the dynamic simulations it is expedient to have an analytical form of the potential. The fitting strategy is as follows. First, for every (θ_i) angular grid point we fit the R-dependence of each adiabatic state to a slightly modified Esposti and Werner[23] function. The modified function has the following form:

$$V(R) = \left[G(R)\, e^{-a_1 R - a_2} - T(R) \sum_{i=6}^{9} \frac{C_i}{R^i}\right] \tag{2}$$

where

$$G(R) = \sum_{j=0}^{8} g_j R^j \tag{3}$$

and

$$T(R) = \frac{1}{2}(1 + \tanh(1 + tR)) \tag{4}$$

is a damping function. The parameters a_i, g_j, t, and C_i have to be optimized for each (θ_i) grid point using the modified Levenberg−Marquardt algorithm from the MINPACK set of routines for the nonlinear least-squares fitting. Having analytical fits for radial variable R we can construct the complete potential by expanding in the series of the reduced Wigner functions $d^l_{m0}(\theta)$. For the sake of dynamical calculations, it is convenient to expand a half of the sum and a half of the difference of the A″ and A′ adiabats to define the so-called V_{sum} and V_{diff} diabats:[24−26]

$$\begin{aligned} V_{sum}(R,\theta) &= \frac{A'' + A'}{2} = \sum_{l=0} v_{l0}(R)\, d^l_{00}(\theta) \\ V_{diff}(R,\theta) &= \frac{A'' - A'}{2} = \sum_{l=2} v_{l2}(R)\, d^l_{20}(\theta) \end{aligned} \tag{5}$$

To obtain $v_{lm}(R)$ radial coefficients for each diabat, the following system of algebraic equations is solved using linear least-squares method:

$$\boldsymbol{T}\mathbf{v} = \mathbf{V}^i_s(R,\theta_i) \tag{6}$$

where the matrix $\boldsymbol{T}$ contains the values of $d^l_{m0}(\theta)$ elements. We have found that it is sufficient to limit the angular expansion in eq 6 to $l_{max} = 9$.

A. Features of Adiabatic and Diabatic PESs. Contours of the adiabatic $^2A'$ and $^2A''$ potential energy surfaces are shown in Figure 2 and 3, respectively. Both the adiabats have global minimum located in the vicinity of $\theta = 90°$ related to a T-shape

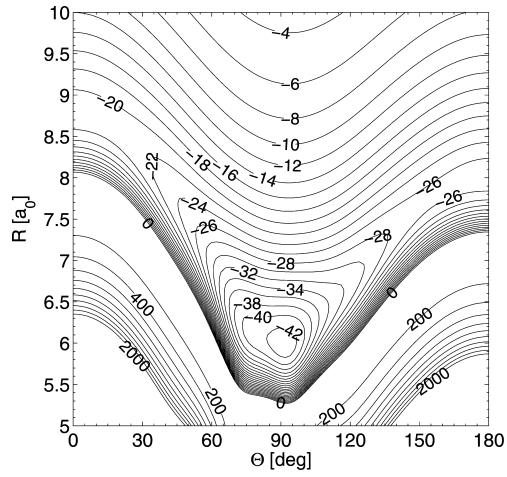

Figure 2. Contour plot of the $^2A'$ adiabatic potential energy surface (in cm^{-1}).

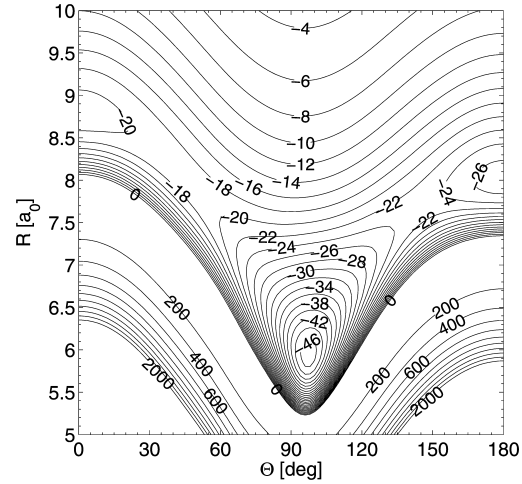

Figure 3. Contour plot of the $^2A''$ adiabatic potential energy surface (in cm^{-1}).

complex. The parameters of the global minimum for the $^2A'$ surface are: $R_e = 5.99$ a_0, $\theta_e = 91.67°$ and $D_e = 43.33$ cm^{-1}. The global minimum for the $^2A''$ surface has the following parameters: $R_e = 5.94$ a_0, $\theta_e = 97.39°$ and $D_e = 47.17$ cm^{-1}. There are local minima or saddle points for the collinear configurations, depending on wether the $^2A'$ or $^2A''$ adiabat is considered. The linear local minimum for $\theta = 0°$ (He···N═C═O) occurs at $R_e = 8.79$ a_0 and is 21.03 cm^{-1} deep. The local minimum located at the O-side of the NCO molecule ($\theta = 180°$) is located at $R_e = 8.02$ a_0 with the well depth of 27.05 cm^{-1}.

The $^2A'$ and $^2A''$ adiabats exhibit similar anisotropy. The interaction energy is practically symmetric with respect to $\theta = 90°$ expressing near-homonuclear character of the NCO molecule. Consequently, the V_{sum} diabatic surface is also approximately symmetric with respect to $\theta = 90°$. The global minimum of the average potential is located at $R_e = 5.98$ a_0 and $\theta_e = 95.42°$ and is 44.66 cm^{-1} deep. In the paper of Macdonald and Liu,[15] the authors deduced characteristic features of the He−NCO PES without prior knowledge of the *ab initio* potentials. They inferred that the average potential should resemble the PES of the He−CO_2 closed-shell system except for a slight asymmetry due to presence of an unpaired electron. Comparing the He−CO_2 PES from the work of Korona et al.[27] with the contour of V_{sum} diabat shown in Figure 4 one can see that, indeed, there is remarkable similarity between the average He−NCO potential and the He−CO_2 potential, the latter being

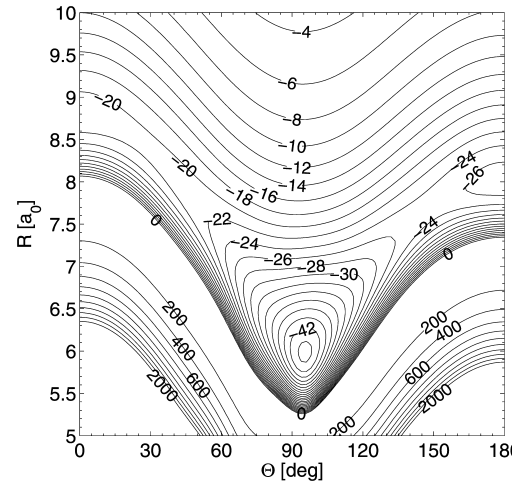

Figure 4. Contour plot of the V_{sum} diabatic potential energy surface (in cm^{-1}).

TABLE 1: Localization and Well Depths of Local and Global Minima for the A′ and A″ Adiabats and V_{sum} Diabat of the He−NCO Complex[a]

PES	R_e/a_0	Θ_e/deg	D_e/cm^{-1}
$^2A'$	5.99	91.67	43.33
$^2A''$	5.94	97.39	47.17
V_{sum}	5.98	95.42	44.66
	8.79	0.00	21.03
	8.02	180.0	27.05
He−CO_2	5.82	90.0	49.31
	8.09	0.00/180.0	26.74

[a] Values corresponding to CCSD(T) results for the He−CO_2 system are taken from Korona *et al.*[27]

only somewhat deeper. Global and local minima of the He−NCO system and related minima for the He−CO_2 system from ref 27 are listed in Table 1. The global minimum of the He−CO_2 PES is located at $\theta = 90°$, similarly to the He−NCO system where the position of the global minimum is only slightly away from strictly perpendicular arrangement of the He atom. Formally, the $\Theta > 90$ part of $^2A''$ He−NCO surface should resemble that of the He−CO_2 closed-shell system. If one compares positions and well depths of minima on the $^2A''$ surface with those on the $^1A'$ He−CO_2 surface in Table 1, one can notice striking resemblance. Macdonald and Liu also deduced that the difference diabat (V_{diff}) would be highly anisotropic, of the shape of "8" relative to the axis along the NCO molecule. They also claimed that the difference potential would be of short-range character. Figure 5 shows the contour plot of the V_{diff} diabatic potential from our *ab initio* calculations. In accord with the empirical hypothesis, the potential is highly anisotropic, has a short-range character, and rapidly decays to zero when R goes to large values, and, last not least, its shape indeed resembles "8".

It is also interesting to compare the He−NCO($X^2\Pi$) potentials to the potentials of He−NO($X^2\Pi$) from Kłos et al.[28] The V_{sum} and V_{diff} diabats for He−NO system reveal the anisotropy similar to the anisotropy of the He−NCO diabats: only the interaction energy in the former case is almost twice as small in the T-shape region. In addition, the V_{diff} diabat shows the opposite sign when comparing to He−NCO system; this is due to the fact that for the He−NO system the A′ state is lower in energy than the A″ state, whereas the reverse is true for He−NCO system.

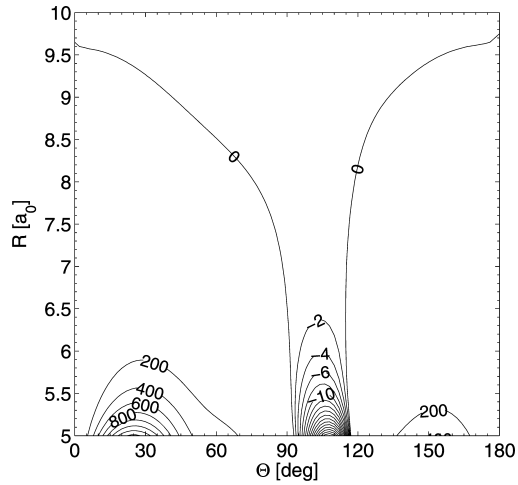

Figure 5. Contour plot of the V_{diff} diabatic potential energy surface (in cm^{-1}).

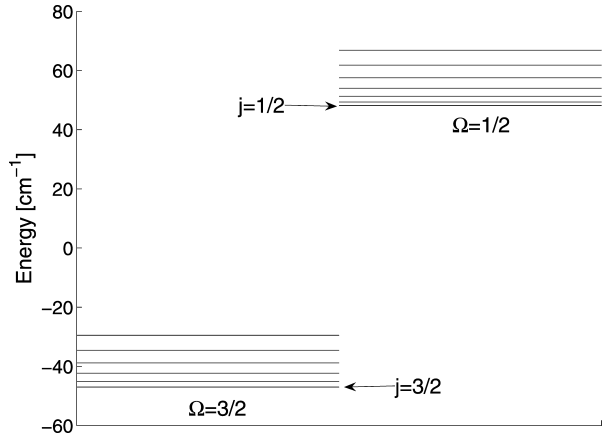

Figure 6. Example of the spectrum of rotational levels of the NCO molecule in the $^2\Pi$ ground electronic state. The F_1 and F_2 spin−orbit manifolds are shown in the real energetic scale, therefore Λ-doublet splittings are not visible.

IV. Scattering Calculations

Theoretical framework for scattering studies of closed shell spherical species with $^2\Pi$ open-shell diatomics was formulated mainly in the early 1980s by Alexander.[29] We can apply the same formalism to a linear triatomic $^2\Pi$ radical in collisions with the He atom. The scattering process of $^2\Pi$ radicals is complicated by an extra degree of freedom of the unpaired electron that adds up to the relative translational motion.

The ground $^2\Pi$ NCO electronic state is split into two spin−orbit manifolds labeled, according to Hund's case (a), as F_1 and F_2. The manifolds are characterized by projection numbers Ω of the total angular momentum of the NCO molecule: the F_1 manifold is related to $\Omega = 3/2$ and the F_2 manifold to $\Omega = 1/2$. This is reciprocal to the NO molecule case, for which the lowest spin−orbit manifold corresponds to $\Omega = 1/2$. The spin−orbit constant of NCO($X^2\Pi$) is $A_{so} = -95.585\ cm^{-1}$,[30] and the rotational constant is $B_e = 0.389516\ cm^{-1}$. The ratio $A_{so}/B_e = -245$ as reported by Macdonald and Liu.[14] In this case we have an almost pure Hund's case (a) for many rotational states because $A_{so} \gg B_e J$. Each rotational level J is additionally split into two closely lying Λ-doublet levels of spectroscopic parity e (symmetry quantum number $\epsilon = +1$) or f ($\epsilon = -1$). The Λ-doubling parameters were set equal to $p = 2.7 \times 10^{-3}\ cm^{-1}$ and $q = -6.2 \times 10^{-5}\ cm^{-1}$.[30] The example of rotational spectrum of the NCO $^2\Pi$ molecule with the spin−orbit structure for the first six rotational levels is shown in Figure 6. The Λ-doublet parity splittings are not visible for this energy scale. These rotational states are indicated below, following Alexander:[29]

$$E_{j,\Omega=3/2,\epsilon} = 1/2A_{so} + B_e[j(j+1) - 7/4] + 1/2\epsilon(B_e/A_{so})(2q + pB_v/A_{so})(j - 1/2)(j + 1/2)(j + 3/2)$$
$$E_{j,\Omega=1/2,\epsilon} = -1/2A_{so} + B_e[j(j+1) + 1/4] + 1/2\epsilon p(J + 1/2) \quad (7)$$

The presence of a structureless scattering partner removes the cylindrical degeneracy of the Π state of NCO creating two adiabatic potential energy surfaces of the A′ and A″ symmetries with respect to reflection in the 4-atomic plane. Alexander[24] and Zeimen *et al.*[25,26] describe the expansion of a potential appropriate for description of van der Waals $^2\Pi$ molecular complexes with a structureless spherical target, cf. section III. The states of the NCO radical can be expanded in the following basis:

$$|\Lambda, S, \Omega, j, m_j\rangle = |\Lambda, S, \Omega\rangle \sqrt{\frac{2j+1}{8\pi^2}} D^{j*}_{m_j,\Omega}(\alpha, \beta, \gamma) \quad (8)$$

where $|\Lambda,S,\Omega\rangle$ describes the electronic angular momentum and spin. The polar Euler angles describe the orientation of the axis containing $\vec{r}$ of the NCO molecule relative to the space-fixed frame. In the case of NCO, $\Lambda = \pm 1$ and $S = 1/2$. The elements of the Wigner D matrix describe the rotations of the NCO radical. The Ω quantum number is the projection of the total angular momentum of the NCO on the molecular axis, and m_j is its projection on the z axis of the space fixed frame. It is useful to define a parity adapted basis set, which contains eigenfunctions of the inversion operator:

$$||\Lambda|, S, \Omega, j, m_j, \epsilon\rangle = 2^{-1/2}(|\Lambda, S, \Omega, j, m_j\rangle + \epsilon|-\Lambda, S, -\Omega, j, m_j\rangle) \quad (9)$$

Using this basis set one can expand the total wave function for the He−NCO system in terms of eigenfunctions of the total angular momentum $\hat{J}$, and substitute it to the Schrödinger equation, thus deriving a set of coupled differential equations (close-coupled equations) for a given collision energy. During calculation we use the reduced mass of the complex $\mu = 3.6543$ amu. The close-coupling equations are propagated in the basis of NCO with j up to 40.5, and cross sections are converged by summing all partial waves up to $J = 150.5$.

Neglecting the off-diagonal Coriolis coupling terms is a less computationally expensive approach, called coupled-states approximation. We will use the full close-coupling method for four values of collision energy while the coupled-state method is applied to scan the dependence of state-resolved cross section in a broader range of collision energies. In the sequel, we will describe the theoretical scattering results and compare them to the experimental data.

A. Close-Coupling Calculations. We used full quantum close-coupling (CC) calculations of state-resolved inelastic cross sections for He−NCO($^2\Pi$) only for the following collision energies $E_{col} \in [328.77,566.60,828.92,1066.75]\ cm^{-1}$. For these

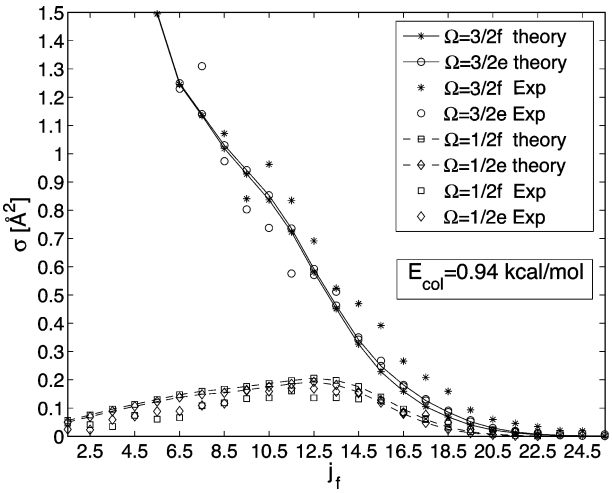

Figure 7. The final fine structure distributions of NCO($^2\Pi$) for collisions with He at the collision energy of 0.94 kcal/mol. The theoretical integral cross sections are calculated with the CC method and averaged over initial Λ-doublet levels. The experimental cross sections[14] were scaled to match the sum of the theoretical cross section for this collision energy.

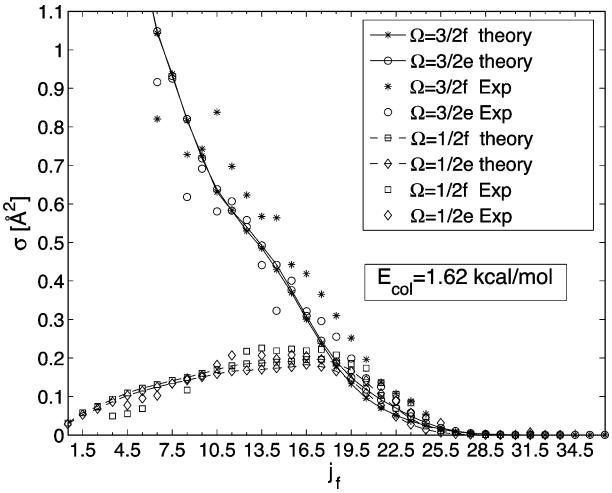

Figure 8. The final fine structure distributions of NCO($^2\Pi$) for collisions with He at collision energy of 1.62 kcal/mol. The theoretical integral cross sections are calculated with CC method and averaged over initial Λ-doublet levels. Experimental cross sections[14] were scaled to match the sum of the theoretical cross section for this collision energy.

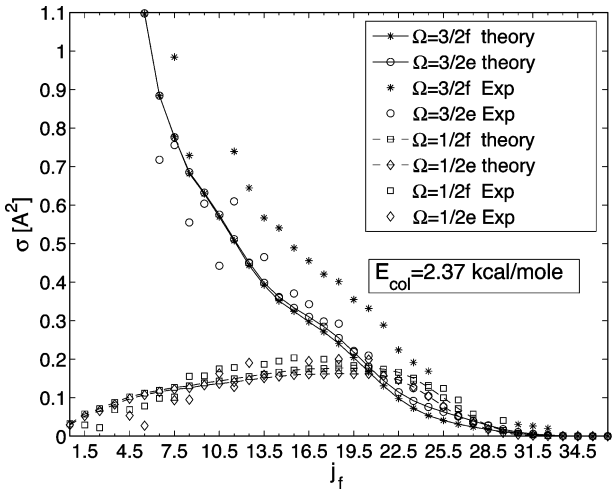

Figure 9. The final fine structure distributions of NCO($^2\Pi$) for collisions with He at collision energy of 2.37 kcal/mol. The theoretical integral cross sections are calculated with the CC method and averaged over initial Λ-doublet levels. Experimental cross sections[14] were scaled to match the sum of the theoretical cross section for this collision energy.

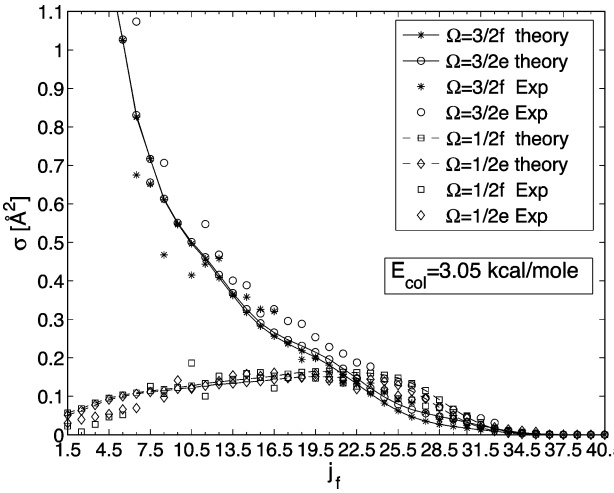

Figure 10. The final fine structure distributions of NCO($^2\Pi$) for collisions with He at collision energy of 3.05 kcal/mol. The theoretical integral cross sections are calculated with CC method and averaged over initial Λ-doublet levels. Experimental cross sections[14] were scaled to match the sum of the theoretical cross section for this collision energy.

values of E_{col} Macdonald and Liu[14] (in their work it is 0.94, 1.62, 2.37, and 3.05 kcal/mol, respectively) performed crossed-beam measurements and reported the fine structure distributions of the scattered NCO. Figures 7, 8, 9 and 10 show the integral cross sections from our CC calculations in comparison with the experimental results of Macdonald and Liu. These cross sections correspond to the following collisional process:

$$\mathrm{NCO}(\mathrm{X}^2\Pi_{3/2}, j = 3/2, e/f) + \mathrm{He}(^1\mathrm{S}) \rightarrow \mathrm{NCO}(\mathrm{X}^2\Pi_{3/2,1/2}, j_f, e/f) + \mathrm{He}(^1\mathrm{S}) \quad (10)$$

The theoretical results are averaged over initial Λ-doublet states. The experimental cross sections are scaled to the theoretical calculations by matching the overall sum of cross sections for both manifolds and the final Λ-doublet states for each collision energy.

The first noticeable characteristic of the cross sections is that those corresponding to the spin−orbit conserving transitions decline monotonically with increasing the final rotational quantum number. This is similar to the behavior of the cross sections for scattering of a closed-shell molecule. It is known that the He−NCO system is very close to a pure Hund's case (a), hence the radial expansion terms of the V_{sum} diabat should be responsible for the spin−orbit conserving transitions. The V_{sum} diabatic PES appears similar to a PES for a closed-shell system. The spin−orbit cross sections reveal a bell-shaped trend with increasing final rotational quantum number. In Hund's case (a) the radial expansion coefficients of the V_{diff} diabat play crucial role in the spin−orbit changing transitions. V_{diff} is very anisotropic and is decaying faster to zero in the long-range than V_{sum}. This causes the spin−orbit changing cross section distributions to be qualitatively different than spin−orbit conserving ones. Following the analysis of Macdonald et al.[14] the bell-shaped distribution of the $\Delta\Omega = 1$ cross sections originates from

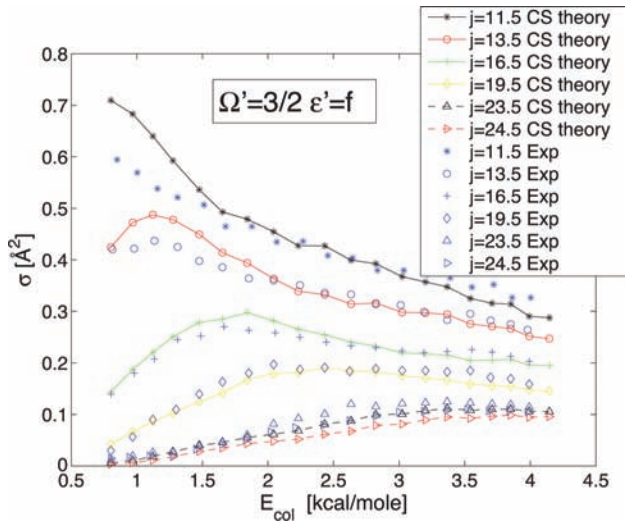

Figure 11. The dependence of the initially Λ-doublet averaged coupled-states and the experimental[14] integral cross sections for several j_f $\Omega' = 3/2$ and $\epsilon' = f$ states on the collision energy. Experimental cross sections were scaled to match the sum of the theoretical cross section.

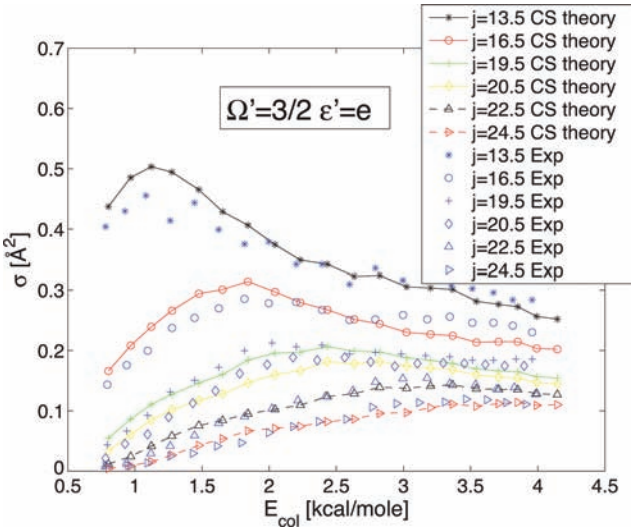

Figure 12. The dependence of the initially Λ-doublet averaged coupled-states and experimental[14] integral cross sections for several j_f $\Omega' = 3/2$ and $\epsilon' = e$ states on the collision energy. Experimental cross sections were scaled to match the sum of all theoretical cross section.

the fact that rotational energy transfer for small values of the final rotational quantum number j_f involves trajectories with a large impact parameter. But for these trajectories the spin−orbit changing probability is the smallest because of the short-range nature of V_{diff}. This results in reduced population for low Δj spin−orbit changing transitions. This theoretical results corroborate the experimental findings of Macdonald et al.[14] They observed the same trends of cross sections for $\Delta\Omega = 0$ and $\Delta\Omega = 1$ transitions.

In Figure 7, we present comparison of theoretical and experimental cross sections for the collision energy of 0.94 kcal/mol. The theoretical cross sections were calculated within the CC framework. The agreement between theoretical and experimental results is very good. The spin−orbit conserving transitions decline in a similar way, both in the theory and the experiment. The theoretical and experimental spin−orbit changing transitions agree very well too: the bell-shaped structure is reproduced, and the experimental and theoretical results start

TABLE 2: Bound States of the He−NCO Complex from Close-Coupling Open-Shell Calculations[a]

J	$n = 1$	$n = 2$	$n = 3$	$n = 4$	$n = 5$	$n = 6$
$1/2^+$	−15.46	−14.26	−7.19	−5.72	−3.86	−2.31
$1/2^-$	−15.56	−14.37	−7.20	−5.73	−3.90	−2.36
$3/2^+$	−15.71	−14.72	−13.53	−12.16	−8.53	−7.20
$3/2^-$	−15.70	−14.70	−13.54	−12.16	−8.53	−7.18
$5/2^+$	−14.92	−14.01	−13.04	−11.86	−10.61	−9.12
$5/2^-$	−14.92	−14.00	−13.01	−11.89	−10.60	−9.13
$7/2^+$	−13.64	−12.92	−11.95	−10.73	−9.60	−8.61
$7/2^-$	−13.63	−12.91	−11.92	−10.72	−9.64	−8.59
$9/2^+$	−11.96	−11.62	−10.61	−9.55	−8.39	−7.21
$9/2^-$	−11.96	−11.61	−10.60	−9.53	−8.41	−7.24

[a] Results are listed for the ground and first four excited states. The total quantum number J runs from $J = 1/2$ to 9/2, and the superscript denotes the total parity p. The label n denotes states in the order of increasing energy. The first few states above the ground state are bending modes, whereas the vibrationally excited mode starts around -3 cm^{-1}. Energies are in cm^{-1}.

TABLE 3: Bound States of the He−NCO Complex from the Coupled-State Approximation Calculations[a]

	$P = 1/2$				$P = 3/2$			
J	(0,0,f)	(0,0,e)	(0,1,f)	(0,1,e)	(0,2,f)	(0,2,e)	(0,3,f)	(0,3,e)
1/2	−14.96	−14.73	−6.75	−6.18				
3/2	−13.92	−13.68	−5.94	−5.40	−14.04	−13.37	−8.05	−6.53
5/2	−12.20	−11.96	−4.62	−4.14	−12.33	−11.64	−6.84	−5.46
7/2	−9.82	−9.58	−2.80	−2.42	−9.96	−9.26	−5.15	−3.99
9/2	−6.83	−6.58	−0.524	−0.318	−7.00	−6.27	−3.02	−2.15
11/2	−3.29	−3.02			−3.54	−2.76	−0.422	

[a] Results are listed for the ground and first three excited states. The total quantum number J runs from $J = 1/2$ to 11/2, and P denotes projection of the total angular momentum quantum number of 1/2 or 3/2. In the parentheses (υ_s,υ_b,ϵ), the quantum numbers for van der Waals stretching (υ_s), bending (υ_b), and parity (ϵ) of symmetrized OH rotor states are denoted. Energies are in cm^{-1}.

to decline in the same range of the final rotational quantum number, approximately around $j_f = 13.5$. The difference between cross sections for $\epsilon = f$ and $\epsilon = e$ transitions is quite small for the theoretical results. This difference for experimental results is similar to the theoretical findings in the case of $\Delta\Omega = 1$ transitions. Interestingly, for the $\Delta\Omega = 0$ transitions the different final Λ-doublet states give cross sections which are more differentiated. Over almost the whole range of final rotational state the spin−orbit changing cross sections are smaller than the spin−orbit conserving ones. The cross sections quickly approach zero for $j_f > 25.5$.

In Figure 8 we show a similar comparison of the integral cross sections for the collision energy of 1.62 kcal/mol. The maximum of the spin−orbit changing cross sections is shifted toward larger Δj in comparison to $E_{\text{col}} = 0.94$ kcal/mol in Figure 7. For $j_f > 19.5$ spin−orbit changing transitions result in slightly larger cross sections than spin−orbit conserving ones. The cross sections become small around $j_f = 35.5$.

In Figures 9 and 10, we show the cross sections for collision energies of 2.37 and 3.05 kcal/mol, respectively. They reveal similar behavior as the above-discussed. The spin−orbit changing cross sections are becoming larger than the corresponding spin−orbit conserving ones for higher values of ΔJ.

B. Coupled-States Scattering Calculations. To calculate dependence of the integral cross sections for the He−NCO collisions on the translational energy we use the less computationally expensive coupled-states (CS) approximation in closed-coupling equations. We calculate cross sections for 20 collision energies between 0.8 and 4.15 kcal/mol. We show the

TABLE 4: Estimates of the Rotational Constant *B* and Centrifugal Distortion Constant *D* for the Ground and the First Two Excited States in the Case of Coupled-States Calculations[a]

	closed shell	$P = 1/2$			$P = 3/2$		
constant	$n = 0$	$n = 0$	$n = 1$	$n = 2$	$n = 0$	$n = 1$	$n = 2$
B_n	0.351	0.349	0.350	0.270	0.347 (0.325)	0.349 (0.327)	0.245 (0.227)
$D \times 10^4$	3.9	3.9	4.0	4.1	4.7	4.4	2.2

[a] The closed-shell CC results for the ground state correspond to calculations in which NCO has no electronic structure and the V_{sum} PES is used. The results in parentheses for the $P = 3/2$ projection quantum number are from the expectation values of the $1/(R^2)$ quantity using corresponding wave functions of the nth excited state for a given P quantum number. Results are in cm^{-1}.

excitation function for $\Delta\Omega = 0$ transition from initial $j = 3/2$ and $\Omega = 3/2$ state. Coupled-states cross sections are averaged over the initial e and f Λ-doublet states. Figure 11 shows a comparison of the theoretical and experimental excitation functions for final states corresponding to $\Omega' = 3/2$ and $\epsilon = f$. Figure 12 shows the same for the $\epsilon = e$ states. In both cases the agreement between theoretical and experimental excitation functions is very good.

The fact that the excitation functions are very well reproduced by using our 2-D potential energy surface indicates that the approximation of NCO as a rigid, inflexible linear molecule is justified.

V. Bound States Calculations

To calculate zero-point corrected dissociation energy we perform calculations of bound states for the He−NCO complex using three different approaches. In the first approach we use the closed-shell approximation in which we treat the NCO as a closed-shell molecule employing only the V_{sum} diabatic surface as the interaction potential. These calculations are performed using program TRIATOM.[31,32] As a second approach we use the collocation method.[33] Both methods give identical results. In the third approach we used the HIBRIDON[34] suite of programs to calculate bound states both within the fully quantum close-coupling scheme and within the coupled-states approximation, allowing for the electronic structure of the NCO radical. The bound states for selected states, characterized by the values of the total angular momentum quantum number ranging from $J = 1/2$ to $J = 9/2$, obtained from the close-coupling open-shell quantum calculations, are listed in Table 2. The zero-point corrected dissociation energy for $J = 3/2$ is 15.7 cm^{-1}, and the total parity splitting is negligible. The potential supports several rovibrational bound states, hence there exists the possibility that the bound He−NCO complex could be observed experimentally in rare-gas matrices. In Table 3, we show the results obtained using coupled-states approximation where Coriolis coupling is neglected; this approximation reduces the dissociation energy by ca. 1 cm^{-1}, therefore the effect of the Coriolis terms although small is noticeable.

Using the following formula:

$$E(J) = E_0 + B \times J(J+1) - D \times [J(J+1)]^2 \tag{11}$$

we estimated rotational constants B and the centrifugal distortion constant D for the first few bound states. The rotational constant of the complex in its ground state is on the order of 0.35 cm^{-1}. In the case of other excited rovibrational states it decreases to 0.25 cm^{-1}. The centrifugal distortion constant is on the order of 4×10^{-4} cm^{-1}.

VI. Summary and Conclusions

We report a potential energy surface for the He−NCO van der Waals system, calculated at the RCCSD(T) level of theory. Our potential is of reduced dimensionality since the NCO molecule is treated as a rigid linear rotor. The global minimum occurs for the T-shape geometry of the $^2A''$ adiabatic surface, and the well is 47.2 cm^{-1} deep. The location of the minimum is close to 90° and separated by 5.9 a_0 from the center of mass of the NCO moiety. The potential reflects a near-homonuclear character of the NCO molecule. In comparison to the He−NO PES of Kłos et al.[28] the He−NCO PES is almost twice as deep in the T-shape region.

The modeled PESs are used in the collisional scattering calculations and the results are compared with the experimental ones of Macdonald and co-workers.[14] The theoretical predictions are in good accord with the integral cross sections and excitation functions experimentally measured, confirming reliability of our PES.

We have estimated the zero-point corrected dissociation energy, D_0, for the He−NCO van der Waals system to be 15.7 cm^{-1}. Using the series of bound state results for different values of the total angular quantum number J, we have estimated the rotational and centrifugal distortion constants. The rotational constant of the complex in the ground state is around 0.35 cm^{-1}.

We conclude that the *ab initio* potentials obtained in this work perform very well in the reproduction of the experimental scattering results, therefore can be recommended to estimate other quantities, i.e., the second virial coefficients, collisional rate constants and many others. The calculations of the collisional rate constants which could be used for modeling of dark interstellar clouds and calculations of the second virial coefficients with quantum corrections are in progress, and will be reported elsewhere.

Acknowledgment. J.K. acknowledges the partial financial support of the University Complutense of Madrid/Grupo Santander under the programme of Movilidad de Investigadores Extranjeros and expresses thanks also for the partial financial support from the U.S. National Science Foundation under Grant CHE-0848110 to M. H. Alexander. G.C. acknowledges financial support of the U.S. National Science Foundation under Grants CHE-0719260 and CHE-0414241.

References and Notes

(1) Wayne, R. P. *Chemistry of Atmospheres*; Clarendon Press: Oxford, 1991.

(2) Cybulski, H.; Zuchowski, P. S.; Fernández, B.; Sadlej, J. *J. Chem. Phys.* **2009**, *130*, 104303.

(3) Kłos, J. A.; Lique, F.; Alexander, M. H. *Chem. Phys. Lett.* **2007**, *12*, 445.

(4) Gredel, R.; van Dishoeck, E. F.; Black, J. H. *Astron. Astrophys.* **1991**, *251*, 625.

(5) Kłos, J.; Lique, F.; Alexander, M. H. *Chem. Phys. Lett.* **2008**, *1*, 445.

(6) Lique, F.; van der Tak, F. F. S.; Kłos, J.; Bulthuis, J.; Alexander, M. H. *Astron. Astrophys.* **2008**, *493*, 557.
(7) Prasad, S. S.; Huntress, W. T. *Mon. Not. R. Astron. Soc.* **1978**, *185*, 741–744.
(8) Iglesias, E. *Astrophys. J.* **1977**, *218*, 697.
(9) Haynes, B. S. *Combust. Flame* **1977**, *28*, 113.
(10) Miller, J. A.; Branch, M. C.; McLean, W. J.; Chandler, D. W.; Smoke, M. D.; Kee, R. J. *Symp. Int. Combust. Proc.* **1984**, *12*, 673.
(11) Wong, K. N.; Anderson, W. R.; Kotlar, A. J.; Vanderhoff, J. A. *J. Chem. Phys.* **1984**, *81*, 2970.
(12) Prasad, R. *J. Chem. Phys.* **2004**, *120*, 10089.
(13) Mladenović, M.; Perić, M.; Engels, B. *J. Chem. Phys.* **2005**, *122*, 144306.
(14) Macdonald, R. G.; Liu, K. *J. Chem. Phys.* **1992**, *97*, 978.
(15) Macdonald, R. G.; Liu, K. *J. Phys. Chem.* **1991**, *95*, 9630.
(16) Macdonald, R. G.; Liu, K. *J. Chem. Phys.* **1993**, *98*, 3716.
(17) Lai, L.-H.; Hui Chiu, Y.; Liu, K. *J. Chem. Phys.* **1995**, *103*, 8492.
(18) Boys, S. F.; Bernardi, F. *Mol. Phys.* **1970**, *19*, 553–566.
(19) Dunning, T. H. *J. Chem. Phys.* **1989**, *90*, 1007.
(20) Misra, P.; Mathews, C. W.; Ramsay, D. A. *J. Mol. Spetrosc.* **1988**, *130*, 419.
(21) MOLPRO is a package of *ab initio* programs written by H.-J. Werner and P. J. Knowles with contributions from R. D. Amos, A. Berning, D. L. Cooper, M. J. O. Deegan, A. J. Dobbyn, F. Eckert, C. Hampel, T. Leininger, R. Lindh, A. W. Lloyd, W. Meyer, M. E. Mura, A. Nicklass, P. Palmieri, K. Peterson, R. Pitzer, P. Pulay, G. Rauhut, M. Schütz, H. Stoll, A. J. Stone and T. Thorsteinsson.
(22) Tao, F. M.; Pan, Y. K. *J. Chem. Phys.* **1992**, *97*, 4989.
(23) Esposti, A. D.; Werner, H.-J. *J. Chem. Phys.* **1990**, *93*, 3351.
(24) Alexander, M.; Stolte, S. *J. Chem. Phys.* **2000**, *112*, 8017.
(25) Zeimen, W. B.; Groenenboom, G. C.; van der Avoird, A. *J. Chem. Phys.* **2003**, *119*, 131–140.
(26) Zeimen, W. B.; Groenenboom, G. C.; van der Avoird, A. *J. Chem. Phys.* **2003**, *119*, 141–148.
(27) Korona, T.; Moszynski, R.; Thibault, F.; Launay, J.-M.; Bussery-Honvault, B.; Boissoles, J.; Wormer, P. E. S. *J. Chem. Phys.* **2001**, *115*, 3074.
(28) Kłos, J.; Chałasiński, G.; Berry, M. T.; Bukowski, R.; Cybulski, S. M. *J. Chem. Phys.* **2000**, *112*, 2195.
(29) Alexander, M. *J. Chem. Phys.* **1982**, *76*, 5974.
(30) Bolman, P. S. H.; Brown, J. M.; Carrington, A.; Kopp, I.; Ramsay, D. A. *Proc. R. Soc. Ser. A, Math. Phys. Sci.* **1975**, *343*, 17–44.
(31) Tennyson, J.; Sutcliffe, B. T. *J. Chem. Phys.* **1982**, *77*, 4061.
(32) Sutcliffe, B.; Tennyson, J. *Int. J. Quantum Chem.* **1991**, *29*, 183.
(33) Cybulski, S. M.; Couvillion, J.; Kłos, J.; Chalasinski, G. *J. Chem. Phys.* **1999**, *110*, 1416.
(34) HIBRIDON is a package of programs for the time-independent quantum treatment of inelastic collisions and photodissociation written by M. H. Alexander, D. Manolopoulos, H.-J. Werner and B. Follmeg, with contributions by P. Vohralik, G. Corey, B. Johnson, T. Orlikowski, P. Valiron and J. Kłos.

JP903918R